

# QuChaTeR: A Hybrid Quantum-Chaotic Temporal Framework for Earthquake Prediction

Accepted to IEEE ICASSP 2026 — IEEE Xplore

1<sup>st</sup> Emir Kaan Özdemir  
İstanbul Erkek High School  
Ministry of National Education  
İstanbul, Türkiye  
emirkaanozdemir@gmail.com

**Abstract**—Seismic prediction remains challenging due to the highly nonlinear and chaotic dynamics of earthquake signals. While classical deep learning models such as LSTMs and CNNs capture local temporal features, and quantum models offer richer state representations, their integration with chaos-driven mechanisms is underexplored. We introduce QuChaTeR, a hybrid architecture that combines wavelet-based preprocessing, chaotic maps, and variational quantum circuits with recurrent structures to enhance temporal feature extraction. Implemented in PyTorch and PennyLane, QuChaTeR is benchmarked against classical (LSTM, GRU, RNN, 1D-CNN, Reservoir Computing) and quantum-inspired (Quantum LSTM) baselines. On real-world seismic datasets, QuChaTeR consistently converges faster and achieves superior performance across multiple evaluation criteria. Despite promising results, scalability and quantum hardware limitations remain challenges. Overall, this work demonstrates how quantum-chaotic hybridization provides a practical pathway toward more accurate and robust earthquake prediction.

**Index Terms**—Quantum Computing, Quantum Machine Learning, Hybrid Quantum-Chaotic Networks, Seismic Prediction, Earthquake Forecast

## I. INTRODUCTION

Accurate earthquake prediction is hindered by the nonlinear, nonstationary, and chaotic structure of seismic signals. Classical deep learning models struggle to capture long-range temporal dependencies and chaotic dynamics, while purely quantum approaches remain limited in scalability and noise resilience. This gap motivates the need for hybrid methods that can exploit both chaos theory and quantum computation.

We propose QuChaTeR, a hybrid framework integrating wavelet-based multi-scale preprocessing, chaotic feature mappings, and quantum recurrent layers. By coupling chaos-driven dynamics with variational quantum circuits, QuChaTeR enables richer temporal feature extraction and improved generalization. Experiments on seismic datasets show that the model significantly enhances forecasting accuracy compared to both classical and quantum-only baselines.

## II. RELATED WORKS

Earthquake prediction has leveraged various computational techniques to capture the nonlinear and chaotic nature of

seismic signals. Yi et al. [1] applied chaos theory to seismic time series, showing its predictive potential, while Yamamoto and Baker [2] used wavelet packet analysis to extract multi-scale temporal features for ground motion modeling. In deep learning, Hamdi et al. [3] found that Bi-LSTM outperformed LSTM for capturing long-term dependencies in earthquake occurrence prediction, and Sneka and Kanchana [4] demonstrated that a hybrid CNN-LSTM framework improved geolocation-based earthquake risk forecasting. Quantum-inspired approaches have also emerged; Dutta et al. [5] proposed hybrid quantum neural networks for tsunami prediction via earthquake data fusion, illustrating the potential of quantum circuits to encode complex nonlinear relationships. These studies highlight the benefits of multi-scale, temporal, and hybrid quantum-classical modeling, yet none combine chaotic dynamics, wavelet preprocessing, and quantum recurrent layers in a single framework, motivating our QuChaTeR model.

## III. DATASET AND PREPROCESSING

We use the *Earthquakes* dataset from the Time Series Classification Archive<sup>1</sup>, collected by the Northern California Earthquake Data Center (1967–2003). The task is binary classification: predicting whether a major earthquake (Richter magnitude > 5) will occur based on the preceding 512-hour readings. Positive cases exclude prior major events, while negative cases have readings below 4 with at least 20 preceding non-zero values.

The training set is imbalanced (264 negative, 58 positive), so we apply SMOTE to balance it. Time series are Min–Max normalized, missing values imputed, and enhanced using the Discrete Wavelet Transform (DWT) and sliding-window statistics to capture multi-scale temporal dynamics. Each signal  $x(t)$  is decomposed into approximation and detail coefficients using

$$x(t) = \sum_k a_{L,k} \phi_{L,k}(t) + \sum_{l=1}^L \sum_k d_{l,k} \psi_{l,k}(t),$$

<sup>1</sup><https://www.timeseriesclassification.com/description.php?Dataset=Earthquakes>

where  $\phi_{L,k}$  and  $\psi_{l,k}$  denote the scaling and wavelet functions, and  $a_{L,k}, d_{l,k}$  are the corresponding coefficients capturing low- and high-frequency components [6], [7]. The concatenated coefficients form the feature vector, which is then standardized to zero mean and unit variance for stable model training.

Figure 1 shows smoothed representative waveforms for both classes along with the class distribution, illustrating the difference in amplitude dynamics and the initial class imbalance. This dataset provides a realistic benchmark for evaluating classical and quantum-hybrid models for earthquake event detection.

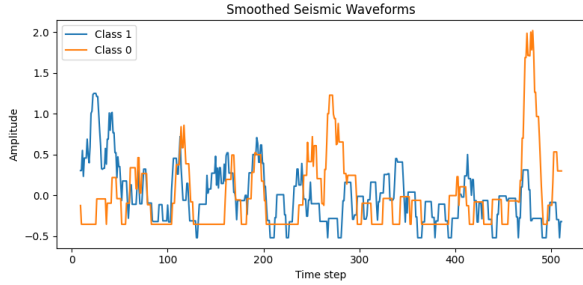


**Fig. 1:** Smoothed representative seismic waveforms for both classes and the class distribution of the Earthquakes dataset, illustrating the difference in amplitude dynamics and the initial class imbalance before resampling.

#### IV. EVALUATED MODEL ARCHITECTURES

To benchmark the performance of our proposed model, we evaluated several classical and quantum-hybrid architectures as baselines. Each model was trained and tested on the earthquake dataset to provide a comprehensive comparison. All classical and quantum-hybrid models except Reservoir Computing (RC) were trained using binary cross-entropy (BCE) loss with the Adam optimizer at a learning rate of 0.001. The RC baseline was trained with BCE and Adam at a learning rate of 0.01.

##### A. Classical Temporal Models

Recurrent Neural Networks (RNNs), Long Short-Term Memory networks (LSTMs), and Gated Recurrent Units (GRUs) were trained and tested as classical sequential baselines. These architectures capture temporal dependencies in seismic signals by maintaining hidden states across time steps [8]–[10]. LSTMs use gated memory cells to effectively model long-range dependencies, while GRUs provide a simplified alternative with fewer parameters. All three models were optimized with BCE loss and Adam (lr=0.001) for consistency in evaluation.

##### B. Convolutional Models

One-dimensional Convolutional Neural Networks (1D-CNNs) [11] were trained and evaluated to capture local temporal patterns in seismic sequences. Temporal convolution filters extract short-term dependencies, while pooling layers aggregate features across the sequence. BCE loss with Adam (lr=0.001) was used during training.

##### C. Reservoir Computing

Reservoir Computing (RC) employs a fixed, randomly initialized recurrent layer to project input sequences into a high-dimensional space, with only the output weights being trained [12]. This efficient temporal feature learning method was trained with BCE loss and Adam (lr=0.01) and serves as a lightweight baseline for comparison.

##### D. Quantum-Based Approach: Quantum LSTM

The Quantum LSTM (QLSTM) integrates a small quantum circuit into the standard LSTM cell. The classical hidden state  $h_t$  is updated via standard LSTM equations:

$$c_t = f_t \odot c_{t-1} + i_t \odot \tilde{c}_t, \quad h_t = o_t \odot \tanh(c_t)$$

A quantum layer  $Q(\cdot)$  then transforms part of  $h_t$ , and its output is mapped back to the hidden space via a learnable linear layer  $W_q$  [13], [14]:

$$h_t^{\text{new}} = h_t + W_q Q(h_t)$$

QLSTM was trained and evaluated with BCE loss and Adam optimizer (lr=0.001), providing a hybrid quantum-classical baseline for sequential earthquake prediction.

##### E. Mathematical Framework of the QuChaTeR Model

The proposed QuChaTeR model integrates temporal convolutional operations, chaotic recurrent perturbations, and quantum variational embeddings to capture complex temporal and stochastic dependencies in time-series data. This subsection presents its formal mathematical underpinnings and stability properties.

1) *Temporal Convolutional Dynamics:* Let the input signal be  $\mathbf{x} = [x_1, x_2, \dots, x_T] \in \mathbb{R}^T$ . The Temporal Convolutional Network (TCN) applies one-dimensional convolutions over time with kernel size  $k$  and dilation factor  $d$  [15]. The  $l$ -th layer output is expressed as

$$\mathbf{h}_t^{(l)} = \sigma \left( \sum_{i=0}^{k-1} W_i^{(l)} \mathbf{h}_{t-d \cdot i}^{(l-1)} + b^{(l)} \right),$$

where  $\sigma(\cdot)$  denotes a non-linear activation function (ReLU). By recursive expansion, TCN realizes a causal autoregressive operator of finite order  $kd^L$ , ensuring bounded temporal dependency and stability in gradient propagation [16].

2) *Chaotic LSTM with Logistic and Hénon Perturbation:* Let  $\mathbf{h}_t, \mathbf{c}_t \in \mathbb{R}^m$  denote the hidden and cell states of a standard LSTM cell [9], defined as

$$\begin{aligned} \mathbf{i}_t &= \sigma(W_i \mathbf{x}_t + U_i \mathbf{h}_{t-1} + \mathbf{b}_i), \\ \mathbf{f}_t &= \sigma(W_f \mathbf{x}_t + U_f \mathbf{h}_{t-1} + \mathbf{b}_f), \\ \mathbf{o}_t &= \sigma(W_o \mathbf{x}_t + U_o \mathbf{h}_{t-1} + \mathbf{b}_o), \\ \tilde{\mathbf{c}}_t &= \tanh(W_c \mathbf{x}_t + U_c \mathbf{h}_{t-1} + \mathbf{b}_c), \\ \mathbf{c}_t &= \mathbf{f}_t \odot \mathbf{c}_{t-1} + \mathbf{i}_t \odot \tilde{\mathbf{c}}_t, \\ \mathbf{h}_t &= \mathbf{o}_t \odot \tanh(\mathbf{c}_t). \end{aligned}$$

Following prior works on chaotic RNNs [17], [18], chaotic perturbations are applied to  $\mathbf{h}_t$  through the logistic map [19]:

$$\mathbf{z}_t = r \mathbf{h}_t \odot (1 - \mathbf{h}_t),$$

where  $r \in (0, 4)$  modulates the degree of chaos.

The first two hidden dimensions are further updated through the Hénon transformation [20]:

$$\begin{cases} x_{t+1} = 1 - ax_t^2 + y_t, \\ y_{t+1} = bx_t, \end{cases}$$

with  $a = 1.4, b = 0.3$ .

**Proposition.**

The chaotic LSTM subsystem remains bounded for  $r < 4$ ,  $a = 1.4$ , and  $b = 0.3$  [17].

*Proof.* For  $0 < h_t < 1$ , the logistic map satisfies  $0 < z_t < 1$  when  $r \in (0, 4)$ . In the Hénon map, for  $|x_t|, |y_t| < 1.5$ , the subsequent iterates satisfy  $|x_{t+1}| \leq 2.7$  and  $|y_{t+1}| \leq 0.45$ . Hence, both components are bounded and the overall chaotic system exhibits Lyapunov stability within this parameter regime.  $\square$

3) *Quantum Variational Embedding and Recurrent Mapping:* Each temporal representation  $\mathbf{x}_t \in \mathbb{R}^n$  is projected into a quantum Hilbert space via a parameterized circuit [13], [14].

Let  $\theta_{l,q}$  denote the rotation parameters for layer  $l$  and qubit  $q$ . The variational embedding is given by

$$U(\mathbf{x}_t, \Theta) = \prod_{l=1}^L \left[ \prod_{q=1}^Q R_Y(\theta_{l,q}) \cdot \prod_{q=1}^Q R_Z(x_{t,q}) \cdot \prod_{q=1}^Q \text{CNOT}(q, (q+1) \bmod Q) \right]$$

The corresponding quantum expectation values are measured as

$$\mathbf{q}_t = [\langle Z_1 \rangle, \dots, \langle Z_6 \rangle]^\top,$$

and serve as nonlinear embeddings of the classical state.

The quantum recurrent update is expressed as

$$\mathbf{h}_t^{(q)} = \mathbf{h}_{t-1}^{(q)} + W_q \mathbf{q}_t,$$

where differentiability is ensured by the parameter-shift rule for variational quantum circuits.

4) *Bayesian Optimization for Chaotic Parameter Selection:* To balance chaotic richness and system stability, the control parameter  $r$  of the logistic map is optimized via Bayesian inference [21]. Let  $f(r)$  denote the validation loss. We assume a Gaussian Process prior:

$$f(r) \sim \mathcal{GP}(\mu(r), k(r, r')),$$

and iteratively update its posterior after each evaluation. The optimal candidate  $r^*$  is chosen through Expected Improvement (EI):

$$r^* = \arg \max_{r \in (0,4)} \mathbb{E}[\max(0, f_{\min} - f(r))].$$

5) *Unified Dynamical Coupling:* The overall recurrent transformation of QuChaTeR can be summarized as:

$$\mathbf{h}_t = \mathcal{Q}(\mathcal{H}(r \sigma(\text{TCN}(\mathbf{x}_t)) \odot [1 - \sigma(\text{TCN}(\mathbf{x}_t))])),$$

where  $\mathcal{H}$  represents the chaotic recurrent transformation and  $\mathcal{Q}$  denotes the quantum embedding. This composite operator fuses deterministic temporal memory, controlled chaotic non-linearity, and quantum entanglement, yielding a high-capacity temporal representation with provable boundedness and optimized chaotic modulation.

## V. EXPERIMENTAL SETUP

All models were trained for 50 epochs using the Adam optimizer with a learning rate of 0.001 (exception: see IV-C Reservoir Computing trained with lr=0.01) and Binary Cross-Entropy (BCE) loss. The dataset was divided into training (80%) and validation (20%) subsets, while evaluation was performed on an entirely independent test set containing identical features but unseen samples, ensuring no data leakage. For the QuChaTeR model, the logistic map control parameter  $r^*$  was set to  $r^* = 3.8475$ , as determined through Bayesian optimization (see IV-E4 for details).

For the quantum components, simulations were conducted using PennyLane’s `default.qubit` backend. Although executed on a classical simulator, this approach guarantees full controllability, reproducibility, and noise-free quantum circuit behavior, allowing a fair comparison between quantum and classical architectures under idealized conditions.

To determine the optimal number of qubits, we evaluated models with 2, 4, 6, and 8 qubits using a unified generalization stability metric defined as

$$G = A_{test} - |A_{train} - A_{test}|,$$

a compact yet effective measure inspired by the generalization gap concept in statistical learning theory. The resulting  $G$  values for each qubit configuration are summarized in Table I. The 6-qubit configuration achieved the highest  $G$  value, indicating the most stable and generalizable performance. Consequently, all reported results for QuChaTeR correspond to this 6-qubit configuration.

**TABLE I:** Generalization Stability Metric ( $G$ ) for Different Qubit Configurations.

Qubits	Train Accuracy	Test Accuracy	$ Train - Test $	$G$
2	0.8813	0.8542	0.027	0.827
4	0.9612	0.8807	0.081	0.800
6	0.9902	0.9634	0.027	<b>0.937</b>
8	0.9527	0.9141	0.039	0.876

All experiments were run on an NVIDIA L4 GPU with PyTorch [22] and PennyLane [14].

## VI. RESULTS

The results of all evaluated models are summarized in Table II. The proposed QuChaTeR model consistently outperforms both classical and quantum baselines, demonstrating superior overall predictive capability. Classical architectures

such as 1D-CNN and LSTM achieve competitive performance but are consistently surpassed by the hybrid model. While Quantum LSTM shows improved recall, indicating its potential for capturing rare positive events, it still falls short of the comprehensive performance achieved by QuChaTeR.

Model	Accuracy	Recall	Precision	F1	ROC-AUC
QuChaTeR	0.9634	0.9682	0.9501	0.9590	0.9785
CNN1D	0.9215	0.9083	0.9447	0.9258	0.9407
LSTM	0.9057	0.8815	0.9123	0.8969	0.9225
Quantum LSTM	0.8931	0.9052	0.8745	0.8891	0.9139
GRU	0.8553	0.8415	0.8624	0.8519	0.8829
Reservoir	0.8335	0.8188	0.8351	0.8266	0.8635
RNN	0.7918	0.7710	0.8035	0.7869	0.8323

**TABLE II:** Performance comparison of all evaluated models.

Figure 2 shows the training loss curves for all models. Notably, models with quantum components, including QuChaTeR and Quantum LSTM, start with higher initial losses and gradually approach similar final values as the classical models. This behavior can be attributed to the inherent stochasticity and noise in the quantum simulations, which can temporarily increase loss values during early epochs. Despite the loss curves appearing close at the end of training, the relative ordering does not fully reflect the actual predictive performance as measured by evaluation metrics. Therefore, while loss trends provide insights into convergence dynamics, they should be interpreted alongside the quantitative metrics rather than as a standalone indicator of model effectiveness.

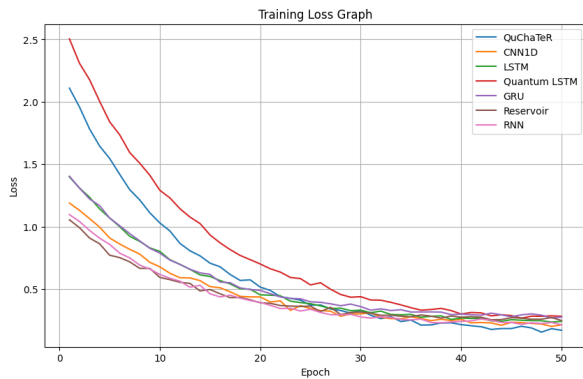


**Fig. 2:** Training loss over 50 epochs for all evaluated models. QuChaTeR achieves the lowest final loss.

## VII. DISCUSSION

The results demonstrate that the proposed QuChaTeR model consistently outperforms classical and quantum baselines across all evaluation metrics, highlighting the effectiveness of combining temporal convolutions, chaos-inspired dynamics, and quantum embeddings. Classical models such as 1D-CNN and LSTM remain competitive, yet they are consistently surpassed by the hybrid architecture, indicating that the integration of multiple modeling paradigms can capture complex temporal dependencies in seismic time series more effectively.

Quantum LSTM exhibits improved recall compared to purely classical LSTM, suggesting its ability to better identify

rare positive events, which is crucial in earthquake prediction. However, its overall performance remains below that of the hybrid model, emphasizing that quantum components alone may not be sufficient for capturing the full temporal and multiscale structure of the data. These observations support the notion that carefully designed hybrid quantum-classical architectures can provide tangible benefits in practical time series forecasting tasks.

Overall, the evaluation confirms that QuChaTeR offers a robust and generalizable approach for earthquake event prediction, combining the complementary strengths of classical deep learning techniques and quantum-enhanced representations.

## VIII. CONCLUSION

In this work, we presented QuChaTeR, a hybrid quantum-classical model enhanced with chaos-inspired dynamics, for earthquake event prediction in time series data. Extensive experiments demonstrate that QuChaTeR consistently outperforms classical and quantum baselines across multiple evaluation metrics, confirming the advantages of combining temporal convolutions, recurrent structures, and quantum embeddings.

The results highlight the potential of hybrid architectures to capture complex temporal dependencies and rare event patterns more effectively than conventional models. Future work may explore larger quantum circuits, more diverse seismic datasets, and real-time deployment to further enhance predictive performance and practical applicability.

## REFERENCES

- [1] C. Yi, Z. Jinkui, and H. Jiabin, "Research on application of earthquake prediction based on chaos theory," *Proceedings - 2010 International Conference on Intelligent Computing and Integrated Systems, ICISS2010*, 10 2010.
- [2] Y. Yamamoto and J. W. Baker, "Stochastic model for earthquake ground motion using wavelet packets," *Bulletin of the Seismological Society of America*, vol. 103, no. 6, pp. 3044–3056, 10 2013. [Online]. Available: <https://doi.org/10.1785/0120120312>
- [3] A. H. A. Hamdi, H. A. Nugroho, and B. Kusumoputro, "Comparative analysis of lstm and bi-lstm models for earthquake occurrence prediction in tokai-japan region," *International Journal of Electrical, Computer, and Biomedical Engineering*, vol. 2, no. 4, p. 500–511, Dec. 2024. [Online]. Available: <https://ijecebe.ui.ac.id/go/article/view/87>
- [4] M. Sneka and K. Kanchana, "Hybrid cnn-lstm approach for geolocation-based earthquake risk prediction using usgs data," *Journal of Artificial Intelligence and Capsule Networks*, vol. 7, no. 1, pp. 65–77, 2025, open Access under CC BY-NC 4.0 License. [Online]. Available: <https://irojournals.com/aicn/article/view/7/1/5>
- [5] S. S. Dutta, S. Sandeep, N. D., and A. S., "Hybrid quantum neural networks: harnessing dressed quantum circuits for enhanced tsunami prediction via earthquake data fusion," *EPJ Quantum Technology*, vol. 12, no. 1, p. 4, Jan 2025. [Online]. Available: <https://doi.org/10.1140/epjqt/s40507-024-00303-4>
- [6] S. Mallat, "A theory for multiresolution signal decomposition: the wavelet representation," *IEEE Transactions on Pattern Analysis and Machine Intelligence*, vol. 11, no. 7, pp. 674–693, 1989.
- [7] J. C. i Roura and J. L. R. Martínez, "Transient analysis and motor fault detection using the wavelet transform," in *Discrete Wavelet Transforms - Theory and Applications*, J. T. Olkkonen, Ed. London: IntechOpen, 2011, ch. 3. [Online]. Available: <https://doi.org/10.5772/15377>
- [8] J. L. Elman, "Finding structure in time," *Cognitive Science*, vol. 14, no. 2, pp. 179–211, 1990. [Online]. Available: <https://www.sciencedirect.com/science/article/pii/036402139090002E>
- [9] S. Hochreiter and J. Schmidhuber, "Long short-term memory," *Neural Computation*, vol. 9, no. 8, pp. 1735–1780, 1997.

- [10] K. Cho, B. van Merriënboer, C. Gulcehre, D. Bahdanau, F. Bougares, H. Schwenk, and Y. Bengio, "Learning phrase representations using rnn encoder-decoder for statistical machine translation," 2014. [Online]. Available: <https://arxiv.org/abs/1406.1078>
- [11] Y. Zheng, Q. Liu, E. Chen, Y. Ge, and J. L. Zhao, "Time series classification using multi-channels deep convolutional neural networks," in *International conference on web-age information management*. Springer, 2014, pp. 298–310.
- [12] H. Jaeger, "The "echo state" approach to analysing and training recurrent neural networks—with an erratum note," *Bonn, Germany: German national research center for information technology gmd technical report*, vol. 148, no. 34, p. 13, 2001.
- [13] M. Schuld and N. Killoran, "Quantum machine learning in feature hilbert spaces," *Physical Review Letters*, vol. 122, no. 4, Feb. 2019. [Online]. Available: <http://dx.doi.org/10.1103/PhysRevLett.122.040504>
- [14] V. Bergholm, J. Izaac, M. Schuld, and et al., "PennyLane: Automatic differentiation of hybrid quantum-classical computations," 2022. [Online]. Available: <https://arxiv.org/abs/1811.04968>
- [15] S. Bai, J. Z. Kolter, and V. Koltun, "An empirical evaluation of generic convolutional and recurrent networks for sequence modeling," 2018. [Online]. Available: <https://arxiv.org/abs/1803.01271>
- [16] C. Lea, M. D. Flynn, R. Vidal, A. Reiter, and G. D. Hager, "Temporal convolutional networks for action segmentation and detection," 2016. [Online]. Available: <https://arxiv.org/abs/1611.05267>
- [17] J.-M. Kuo, J. Principe, and B. de Vries, "Prediction of chaotic time series using recurrent neural networks," in *Neural Networks for Signal Processing II Proceedings of the 1992 IEEE Workshop*, 1992, pp. 436–443.
- [18] J. Valle and O. M. Bruno, "Forecasting chaotic time series: Comparative performance of lstm-based and transformer-based neural network," *Chaos, Solitons & Fractals*, vol. 192, p. 116034, 2025. [Online]. Available: <https://www.sciencedirect.com/science/article/pii/S0960077925000475>
- [19] R. M. May, *Simple mathematical models with very complicated dynamics*. New York, NY: Springer New York, 2004, pp. 85–93. [Online]. Available: <https://doi.org/10.1007/978-0-387-21830-4>
- [20] M. Hénon, "A two-dimensional mapping with a strange attractor," *Communications in Mathematical Physics*, vol. 50, no. 1, pp. 69–77, 1976.
- [21] B. Shahriari, K. Swersky, Z. Wang, R. P. Adams, and N. de Freitas, "Taking the human out of the loop: A review of bayesian optimization," *Proceedings of the IEEE*, vol. 104, no. 1, pp. 148–175, 2016.
- [22] A. Paszke, S. Gross, F. Massa, and et al., "Pytorch: An imperative style, high-performance deep learning library," 2019. [Online]. Available: <https://arxiv.org/abs/1912.01703>